SURGE LINE STRESS DUE TO THERMAL STRATIFICATION

MYUNG JO JHUNG* and YOUNG HWAN CHOI
Korea Institute of Nuclear Safety
19 Guseong-dong, Yuseong-gu, Daejeon, 305-338 Korea
*Corresponding author. E-mail : mjj@kins.re.kr

Received November 5, 2007
Accepted for Publication January 28, 2008

If there is a water flow with a range of temperature inside a pipe, the warmer water tends to float on top of the cooler water because it is lighter, resulting in the upper portion of the pipe being hotter than the lower portion. Under these conditions, such thermal stratification can play an important role in the aging of nuclear power plant piping because of the stress caused by the temperature difference and the cyclic temperature changes. This stress can limit the lifetime of the piping, even leading to penetrating cracks. Investigated in this study is the effect of thermal stratification on the structural integrity of the pressurizer surge line, which is reported to be one of the pipes most severely affected. Finite element models of the surge line are developed using several element types available in a general purpose structural analysis program and stress analyses are performed to determine the response characteristics for the various types of top-to-bottom temperature differentials due to thermal stratification. Fatigue analyses are also performed and an allowable environmental correction factor is suggested.

KEYWORDS : Surge Line, Thermal Stratification, Equivalent Stress, Environmental Fatigue

1. INTRODUCTION

If two media with different densities (e.g., with different temperatures) flow inside a pipe, thermal stratification can occur. For example, warm water is lighter than cool water and therefore tends to float on top of cooler heavier water, resulting in the upper portion of a pipe being hotter than the lower portion. Under these conditions, differential thermal expansion of the pipe metal can cause the pipe to deflect significantly. Unexpected piping movements are highly undesirable because of the potential for high piping stress that may exceed design limits for fatigue and stress. The problem can become more acute when piping expansion is restricted, such as through contact with pipe whip restraints. Plastic deformation can result, which can lead to high local stress, low cycle fatigue and functional impairment of the line.

According to international operating experiences, the material fatigue of nuclear power plant piping caused by thermal stratified flows may limit the lifetime of the pipes [1, 2]; therefore, the consideration of thermal stratification is crucial in the management of plant aging and for extension of the lifetime of nuclear power plants. In pressurized water reactors, thermal stratification is most likely to occur at the feed water lines of the steam generator, at the pressurizer surge line and at the injection pipes of the emergency core cooling systems. Cracks due to stratification were found in the US, France, Belgium, Finland, Japan, etc [3]. The pipe most affected by thermal stratification is reported to be the pressurizer surge line.

In the US, no cracking events have occurred on the pressurizer surge line or at the nozzles. The Trojan plant reported unexpectedly high piping displacements due to thermal stratification, which resulted in crushed insulation, closing of gaps at rupture restraints, and increased pipe support loads. The displacements caused plastic stress and permanent deformation. Beaver Valley 2 also found larger-than-expected piping displacements, which caused snubbers to stroke out. In Slovakia, a surge line elbow at Bohunice 3 was replaced in 2003 due to a high calculated value of cumulative fatigue usage factor [3].

The effect of thermal stratification on the structural integrity of the pressurizer surge line is therefore investigated in this study. Finite element models of the surge line were developed using several element types available in a general purpose structural analysis program and stress analyses were performed to obtain response characteristics for the various types of top-to-bottom temperature differentials due to thermal stratification. Also, environmental fatigue characteristics are addressed for the determination of the mechanical effects of the stratified flow.

2. THERMAL STRATIFICATION IN SURGE LINES

During the operation of the pressurizer heaters, the high temperature medium of the pressurizer expands and flows into the surge line. This warmer coolant can stratify on top of the lower temperature coolant in the surge line and flow above the cooler layer toward the main coolant loop.

During normal operation, the pressurizer heaters periodically operate with a higher temperature than that of the coolant in the main coolant loop hot leg. There is an alternating flow with very low coolant velocities in the surge line in both directions. The heating of the primary circuit during reactor start-up is managed in part with the pressurizer heaters, which means that they operate almost continuously. Therefore, the temperature of the pressurizer is always higher than that of the main coolant loop, so there is a slow but constant flow downward from the pressurizer during the heat-up period. As the hot water flows (at a very low flowrate) from the pressurizer through the surge line to the hot leg piping, the hot water rides on a layer of cooler water, causing the upper part of the pipe to be heated to a higher temperature than the lower part. The temperature differential could be as high as 150°C, based on expected conditions during typical plant operations [2].

3. ANALYSIS

3.1 Finite Element Model

Three finite element models were developed as shown in Fig. 1 using an elastic pipe element (PIPE16), an elastic shell element (SHELL63) and a 3-dimensional structural solid element (SOLID45). PIPE16 is a uniaxial element with tension-compression, torsion, and bending capabilities. The element has six degrees of freedom at two nodes: translations in the nodal x, y, and z directions and rotations about the nodal x, y, and z axes. SHELL63 has both bending and membranous capabilities. Both in-plane and normal loads were permitted. The element has six degrees of freedom at each node: translations in the nodal x, y, and z directions and rotations about the nodal x, y, and z axes. SOLID45 was used for the 3-dimensional modeling of solid structures. This element is defined by eight nodes having three degrees of freedom at each node: translations in the nodal x, y, and z directions.

The finite element model using the solid element has three element layers in the radial direction and therefore has a total of 24336 nodes and 18252 elements. The numbers of nodes and elements are 6444 and 6444 for the shell element model, and 169 and 168 for the pipe element model, respectively.

The boundary conditions at both ends were fixed for all analysis and it was assumed that there were no supports along the line, which is not the case in real systems. In

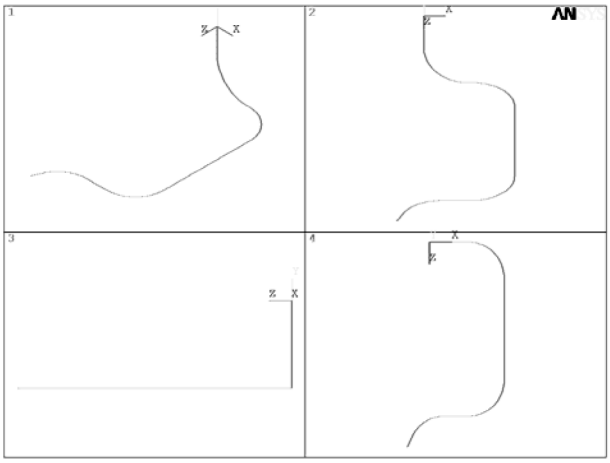

(a) pipe element

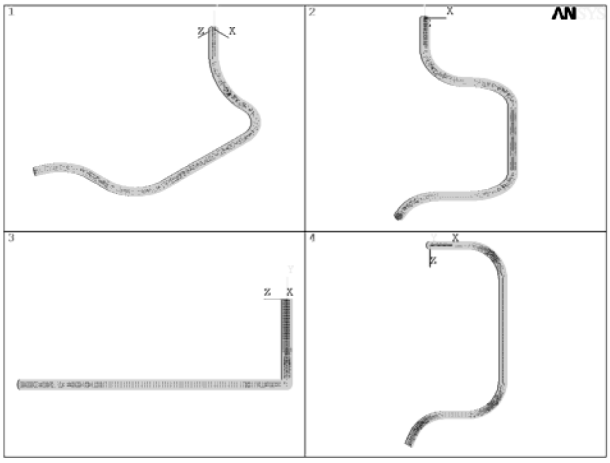

(b) shell element

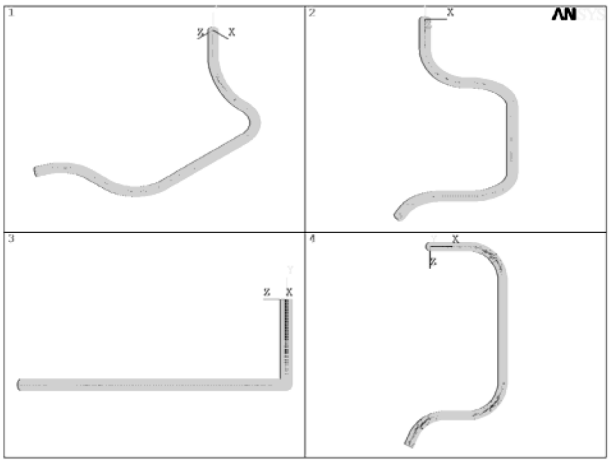

(c) solid element

Fig. 1. Finite Element Models

actual systems, there are 3 variable springs and 4 mechanical snubbers that restrict the movement of the surge line and may generate possible plastic deformation due to abnormal operating conditions. The total mass comparisons between three element models are 3794 kg, 3788 kg and 3773 kg for pipe, shell and solid models, respectively, which is within 0.6% difference.

3.2 Modal Analysis

Modal analyses using a commercial computer code ANSYS [4] were performed to find the vibration characteristics of the surge line. Three different kinds of finite element models were developed for various element types where the surge line was modeled using pipe, shell and solid elements.

The Block Lanczos method [5] was used for the eigenvalue and eigenvector extractions to calculate the natural frequencies of the surge line. It uses the Lanczos algorithm where the Lanczos recursion is performed with a block of vectors. This method is as accurate as the subspace method, and faster. The Block Lanczos method is especially powerful when searching for eigenfrequencies in a given part of the eigenvalue spectrum of a given system. The convergence rate of the eigenfrequencies will be about the same when extracting modes in the midrange and higher end of the spectrum as when extracting the lowest modes.

Modal analyses for the three kinds of finite element models were performed and their first 6 mode shapes are shown in Fig. 2. The frequency comparisons between element types are shown in Fig. 3 and indicate that all three of the element types simulate the model dynamics correctly, which verifies the validity of the finite element models developed for further stress analysis.

3.3 Stress Analysis

A stress analysis for an internal pressure of 10 MPa was performed to determine the stress distributions in the surge line. The equivalent stress and deflection comparisons between element types are shown in Fig. 4 where the maximum stresses are found in the nozzle that connects the surge line with the pressurizer.

As shown in Fig. 4, there are differences of stress between the element types. When comparing results for the pipe element and the shell or solid elements, large differences of stress and deflection exist for all surge line sites such as nozzles and elbows. In ANSYS, the pipe element (PIPE16) was assumed to have “closed ends” so that the axial pressure effect would be included. If the endcap effect is included in the analysis, the maximum stress decreases [6]. This is why the pipe element yields lower stress than the shell or solid element models. When comparing results between the shell and solid elements, there is little difference in the maximum stress and deflection values. In ANSYS, the shell element (SHELL63) had six DOFs, in 3 translations and 3 rotations, but the solid

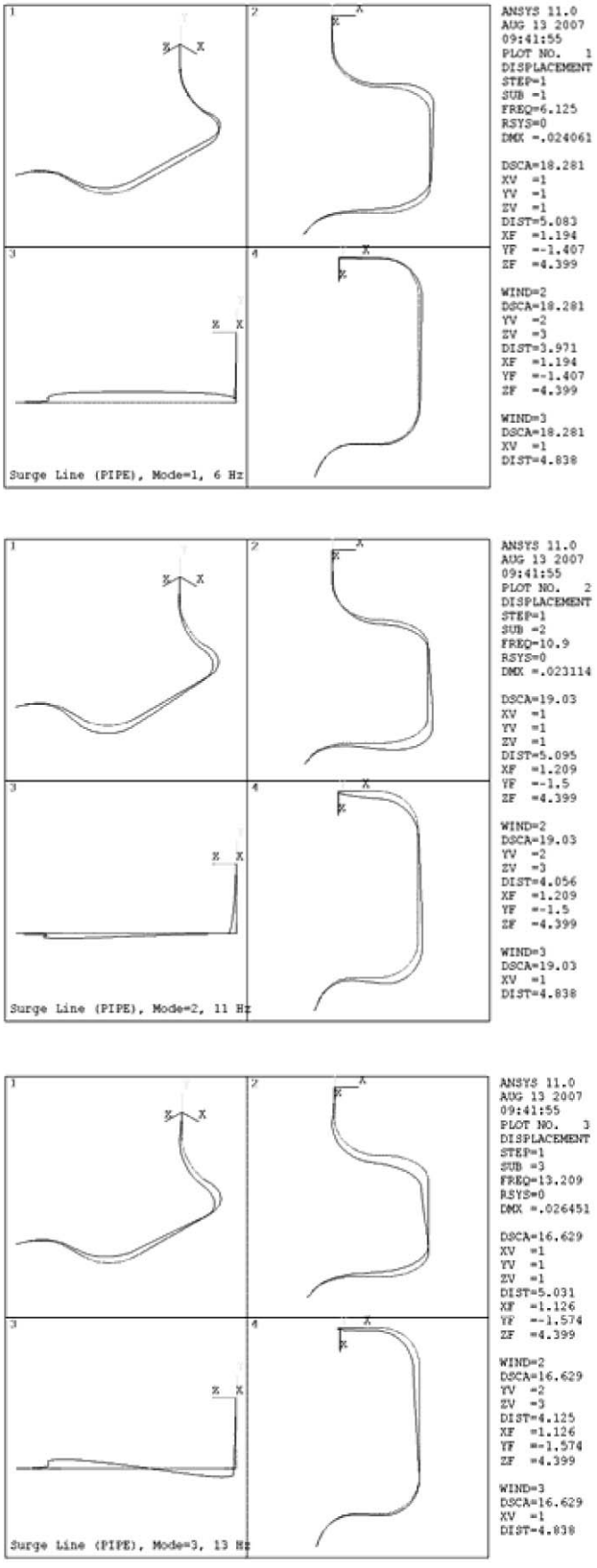

Fig. 2. Mode Shapes of Surge Line

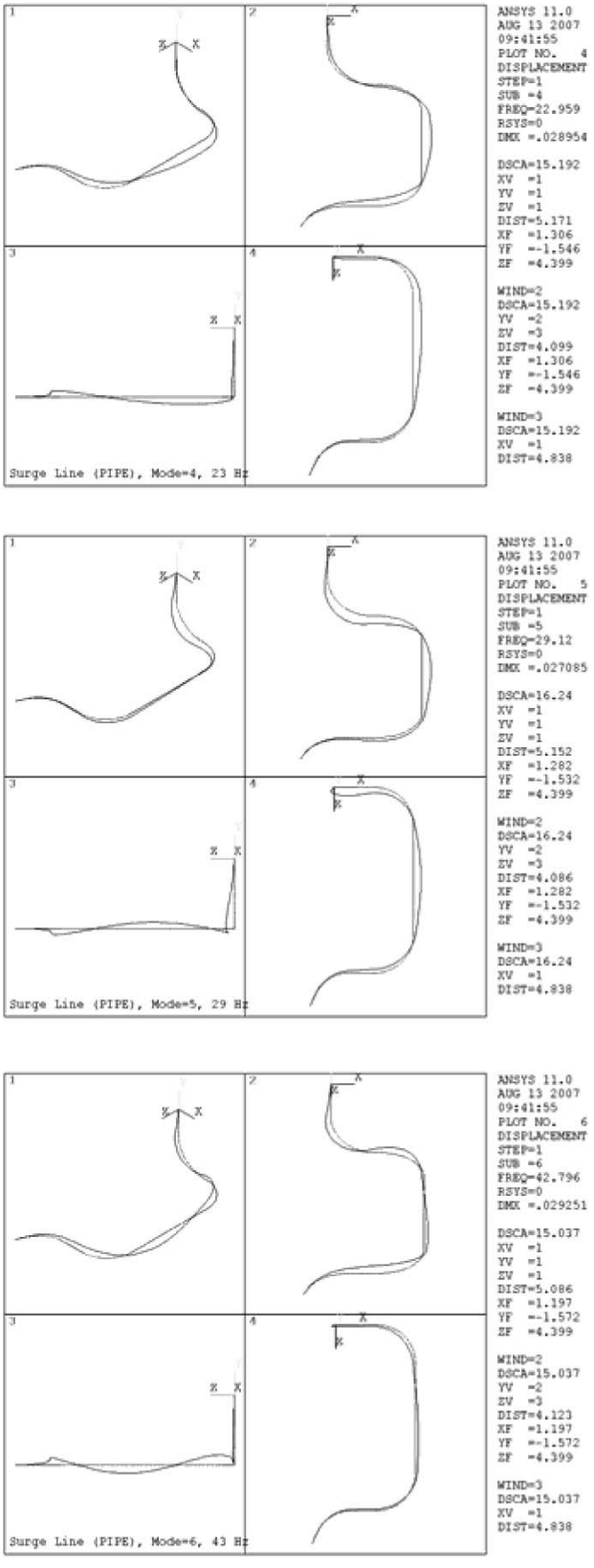

Fig. 2. Mode Shapes of Surge Line (Cont'd)

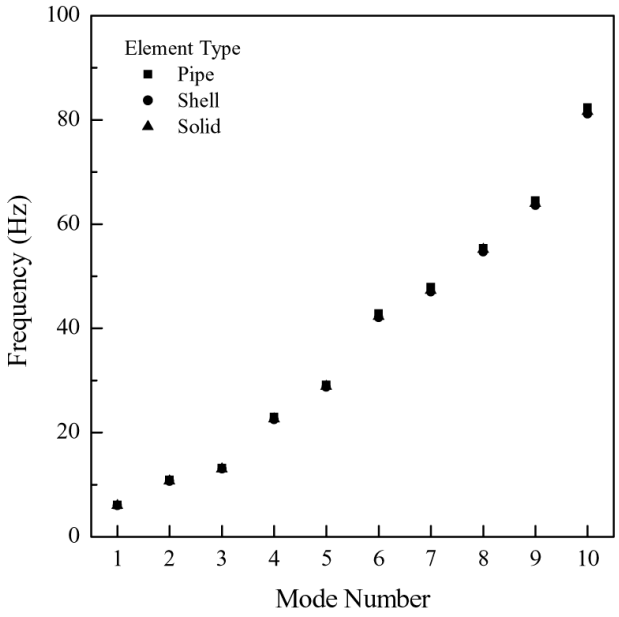

Fig. 3. Frequency Comparisons between Element Types

element (SOLID45) had just three DOFs, in 3 translations. Having different fixed boundary conditions at both ends for the shell and solid models generated different stress at boundaries such as nozzles. The stress of the elbows, which are located far away from the boundary, is almost the same. This was verified from additional analysis applying the same boundary conditions to the shell element where only the translations were fixed at both ends. Although a 4-node finite strain shell element (SHELL181), suitable for analyzing thin to moderately thick shell structures, can be used, it does not produce a good result. The reactions for internal pressures yield results similar to those shown for stress.

An analysis of the stress due to thermal stratification was performed to determine stress distributions in the surge line. Temperature distributions in the surge line were obtained from the thermal hydraulic analysis and were used as an input to the structural analysis. In this study, the temperature was presumed to apply to the lower half and upper half of the pipe by the top-to-bottom temperature differential ΔT, which shows the temperature distributions of $\Delta T = 50°C$. If the exact temperature distributions were available for thermal hydraulic analysis, more accurate stress could be obtained by eliminating conservatism. The equivalent stress comparisons between element types are shown in Fig. 5 where the maximum stresses are found in the nozzle that connects the surge line with the pressurizer.

As shown in Fig. 5, there are differences for stresses between element types. When comparing results for the pipe element and the shell or solid elements, large

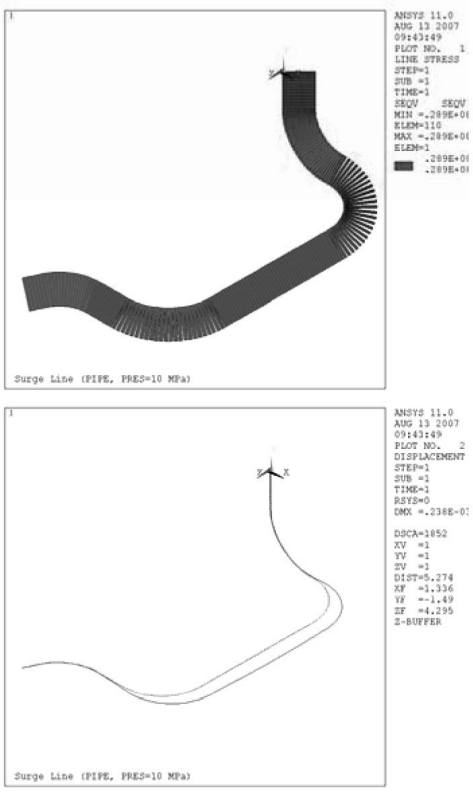

(a) Pipe Element

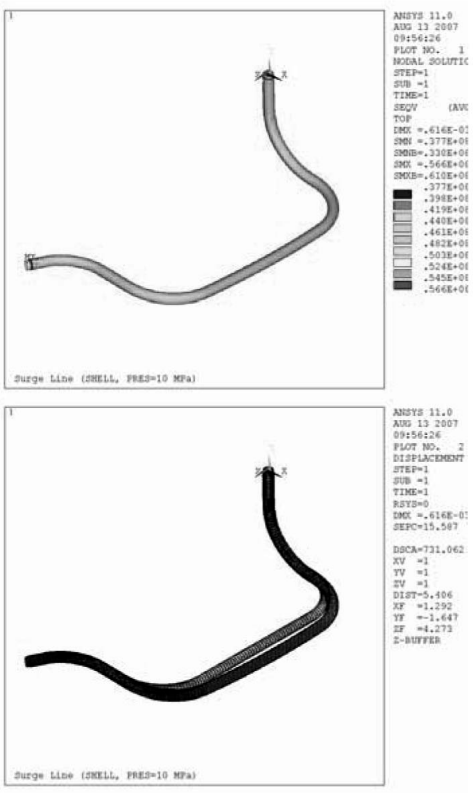

(b) Shell Element

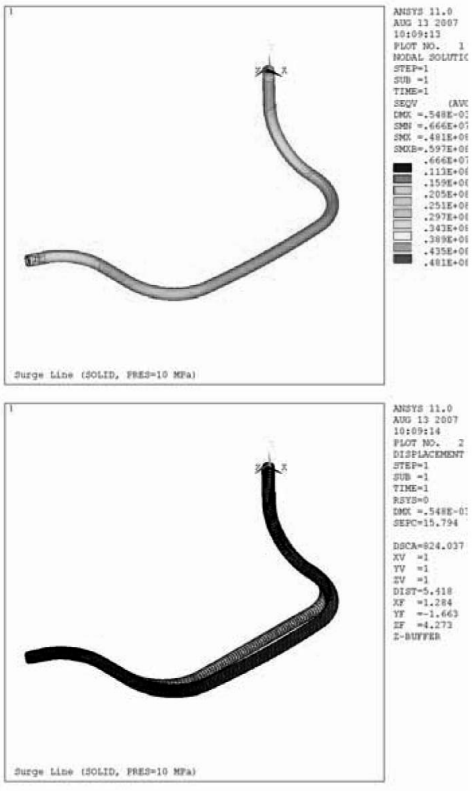

(c) Solid Element

Fig. 4. Equivalent Stresses and Deformations for Internal Pressure

differences of stress and deflection exist for all surge line elements such as nozzles and elbows. In ANSYS, temperature loads for the pipe element were input as element body loads at the nodes at only four points along the circumference, as shown in Fig. 6. Therefore, the temperature is not defined in as much detail as in the shell or solid elements. This may lead to the pipe element model generating different stresses from the shell or solid element models.

Little difference exists between the maximum values for stress and deflection in the shell and solid elements. In ANSYS, the shell element (SHELL63) has six DOFs-3 translations and 3 rotations-but the solid element (SOLID45) has only three DOFs, in 3 translations. Therefore, the fixed boundary conditions at both ends yield different boundary conditions for the shell and solid models, which generate the different stresses at boundaries such as nozzles. The stresses of the elbows, which are located far away from the boundary, are almost the same.

4. RESULTS AND DISCUSSION

Temperature loads for the pipe element were input at

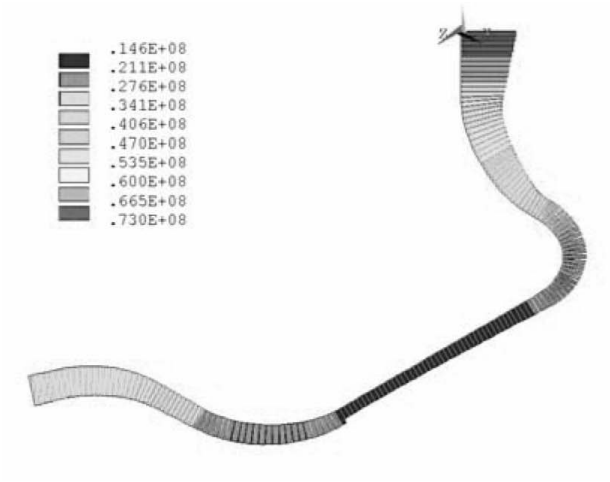

(a) pipe element

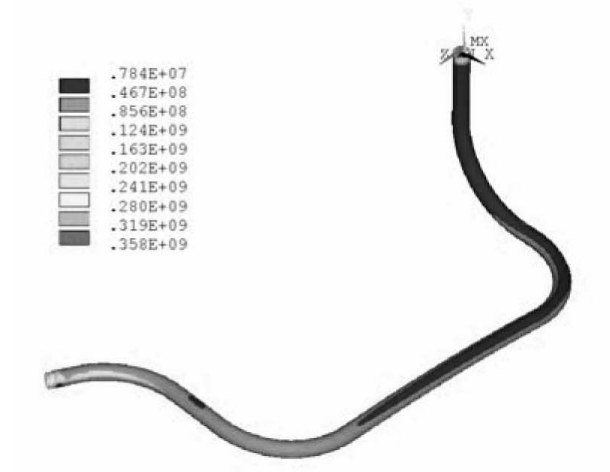

(b) shell element

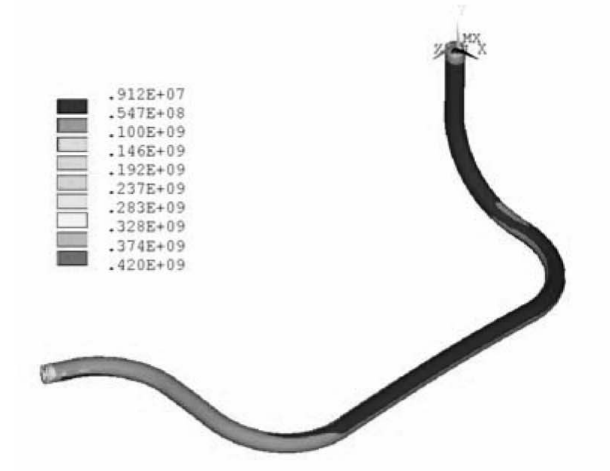

(c) solid element

Fig. 5. Equivalent Stresses for Thermal Stratification

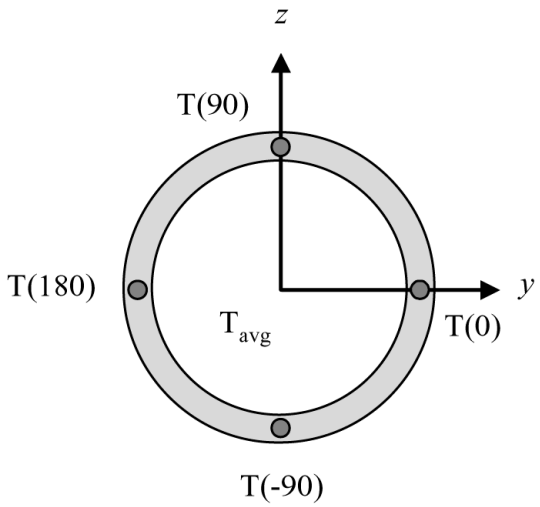

Input : T_{avg}, T(90), T(180)
$T(0) = 2 \times T_{avg}$-T(180)
$T(-90) = 2 \times T_{avg}$-T(90)

Fig. 6. Definition of Temperature Loads in Pipe Element

only four points, and therefore the temperature was not applied in as much detail as in the shell or solid elements that had diametral gradients along their circumferences. As shown in Fig. 6, the average wall temperature of the node (T_{avg}), the average wall temperatures at 90° (T(90)) and at 180° (T(180)) were input for one node, and the temperatures at another two points, 0° and -90°, were computed internally as $2 \times T_{avg}$-T(180) and $2 \times T_{avg}$ - T(90), respectively.

A sensitivity study of temperature loads for various pipe elements due to thermal stratification was performed to obtain the stresses for different temperature loadings at four points. The equivalent stresses and deflections are shown in Fig. 7, where large differences were generated according to the temperature application along the circumference. Therefore, care should be taken in a pipe element to apply temperatures at four points using T_{avg}, T(90) and T(180) inputs, which can be defined based on the element coordinate system orientation.

Using the solid model of the surge line, a sensitivity study was performed for thermal stratification, where three kinds of temperature distribution in the circumferential direction were considered as shown in Fig. 8. Also, one other case of temperature distribution along the length of the surge line was considered as shown in Fig. 9, where the temperature was continuously changed from the hot

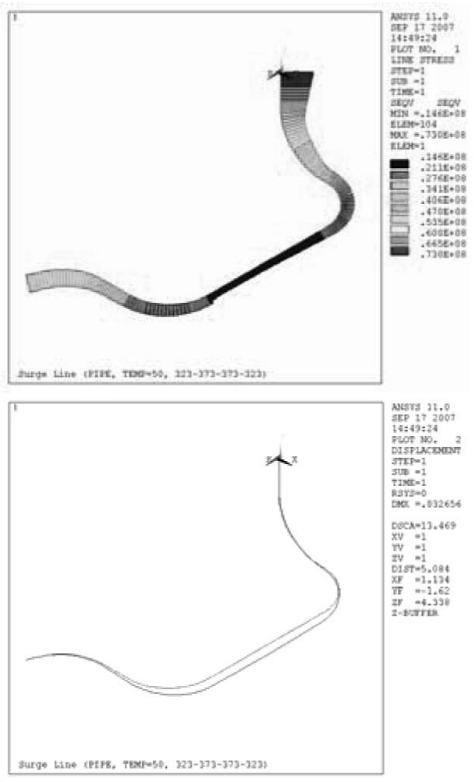

(a) 323-373-373-323

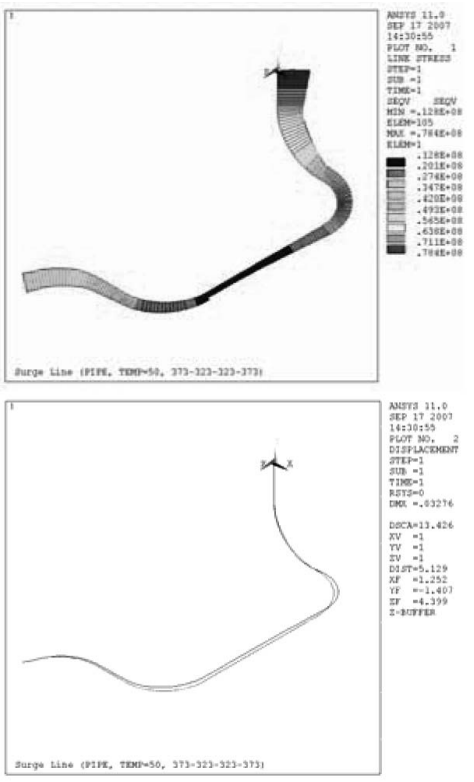

(b) 373-323-323-373

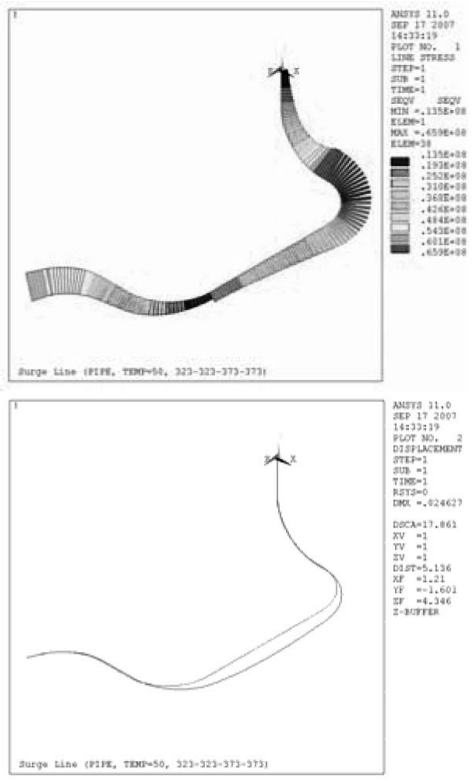

(c) 323-323-373-373

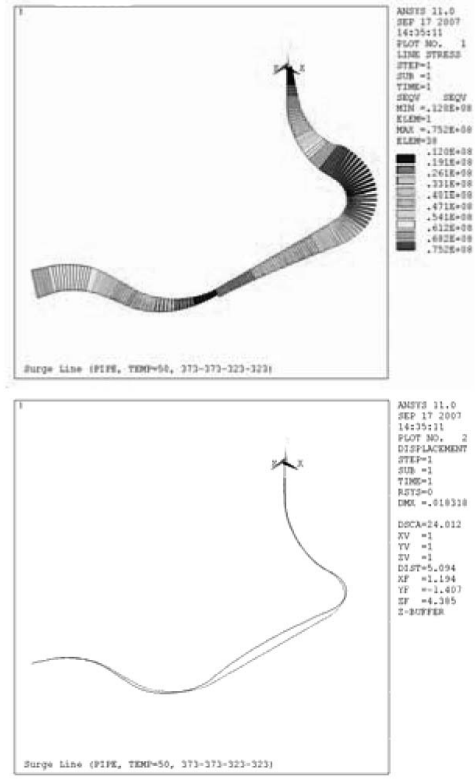

(d) 373-373-323-323

Fig. 7. Equivalent Stresses and Deformations (Numbers are Temperatures Applied to 4 Points of Pipe Element in Fig. 6)

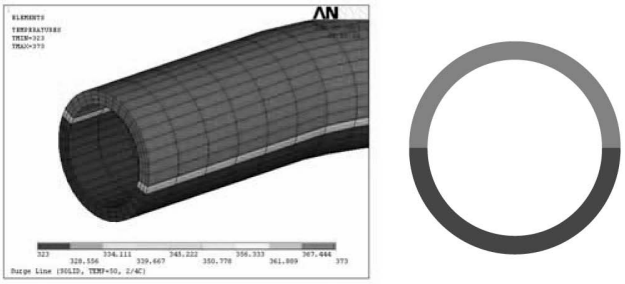

(a) Cool Area - Lower Half

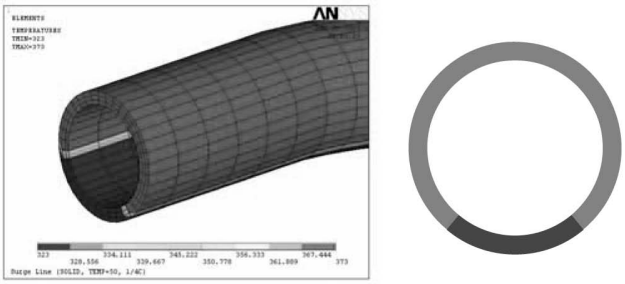

(b) Cool Area - Lower Quarter

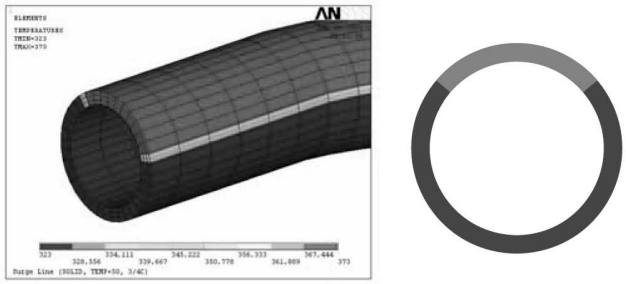

(c) Cool Area - Lower Three Quarters

Fig. 8. Temperature Distributions in the Circumferential Directions

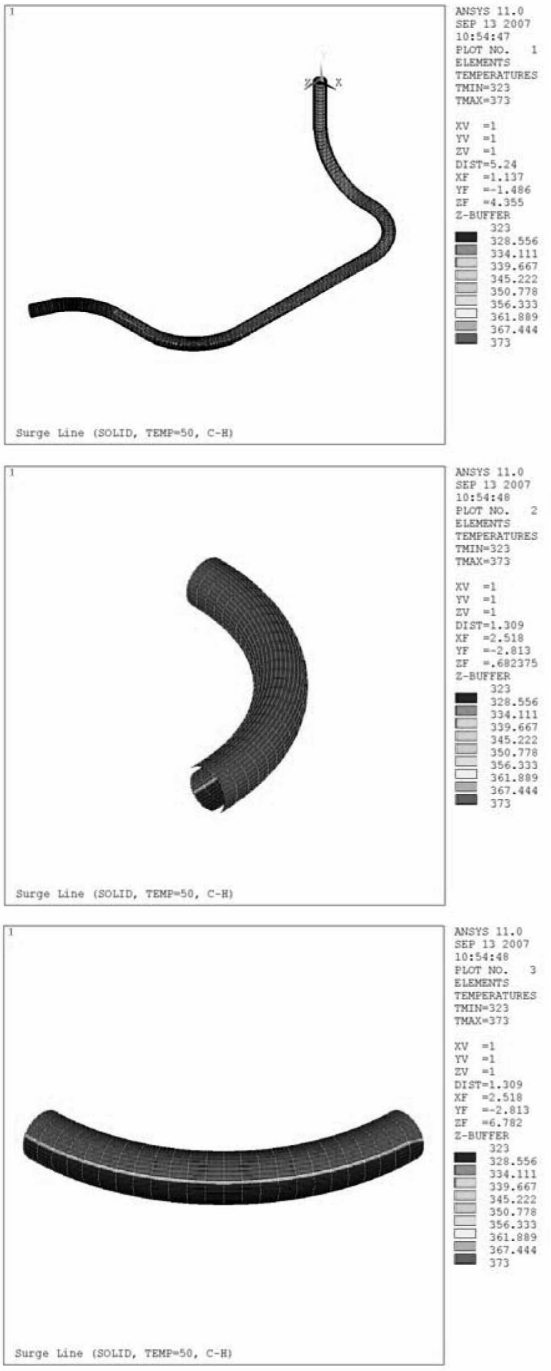

Fig. 9. Temperature Distributions along the Length

leg to the pressurizer with a step change along the length.

The equivalent stresses are shown in Fig. 10, where it is shown that the bottom nozzle of the pressurizer is the most stressed region. Comparisons of equivalent stresses and deflections between temperature loadings are made in Fig. 11. There is little difference in the stress, but much difference in the deflection due to temperature loading. For all cases, upper-half and lower-half distribution of the top-to-bottom temperature differential in the pipe yields the most conservative results.

Stress analyses were performed to determine the pressure and thermal stresses of the surge line. Upper-half and lower-half distribution of the top-to-bottom temperature differential in the pipe, which gave the most conservative results, was applied along with the internal pressure of 10 MPa to generate normal operating stresses.

The equivalent stresses and deflections due to thermals stratification of $\Delta T = 50°C$ and the internal pressure of 10 MPa are shown in Fig. 12. As shown in Fig. 12, the stress due to thermal stratification is much higher than that due to internal pressure and thermal stratification is

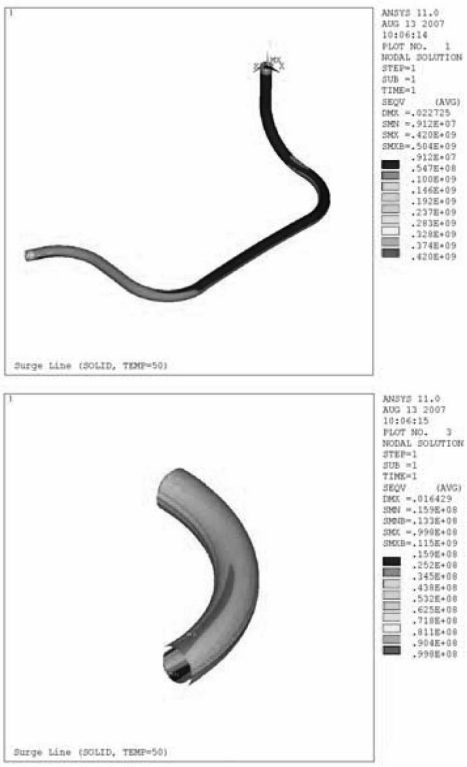

(a) 2/4Hot, 2/4Cool

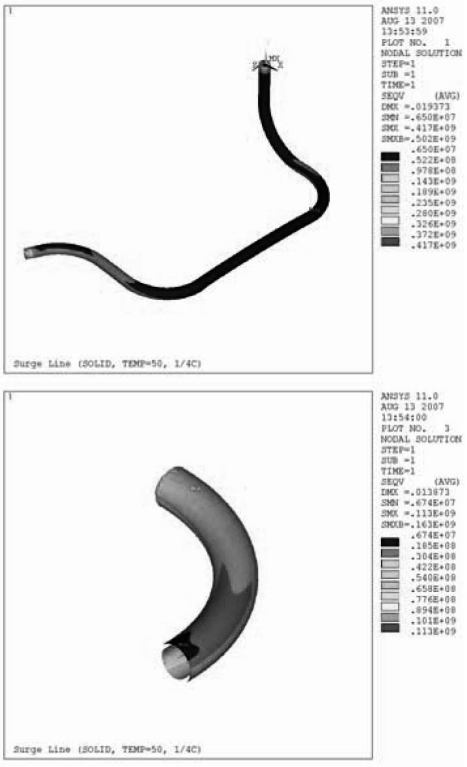

(b) 3/4Hot, 1/4Cool

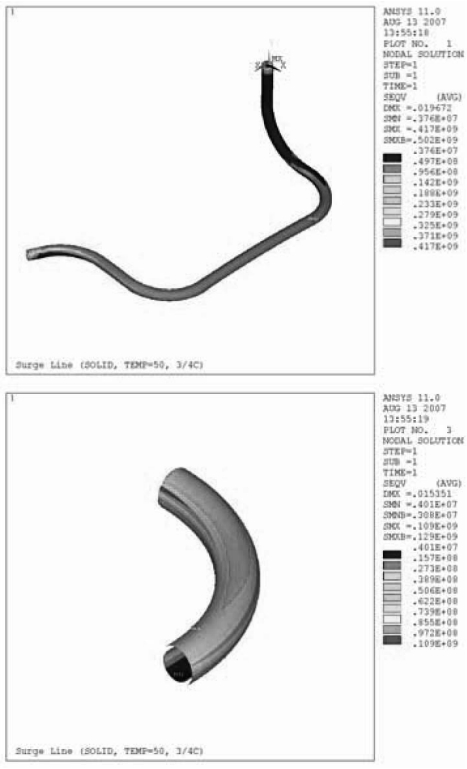

(c) 1/4Hot, 3/4Cool

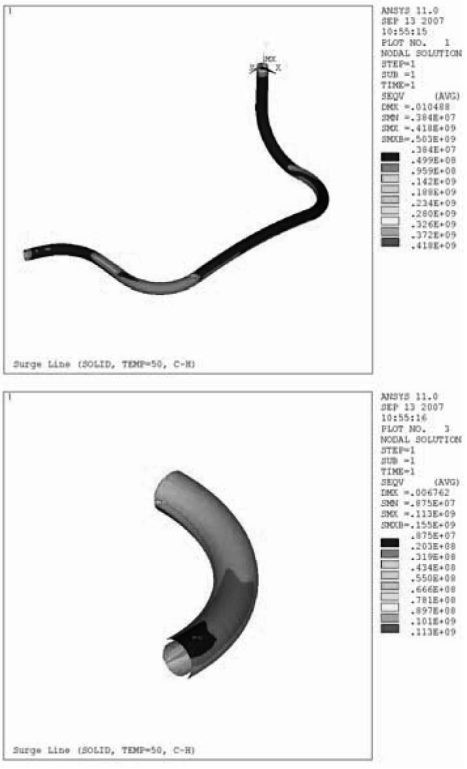

(d) Hot-Cool

Fig. 10. Equivalent Stresses for Various Temperature Distributions due to Thermal Stratification

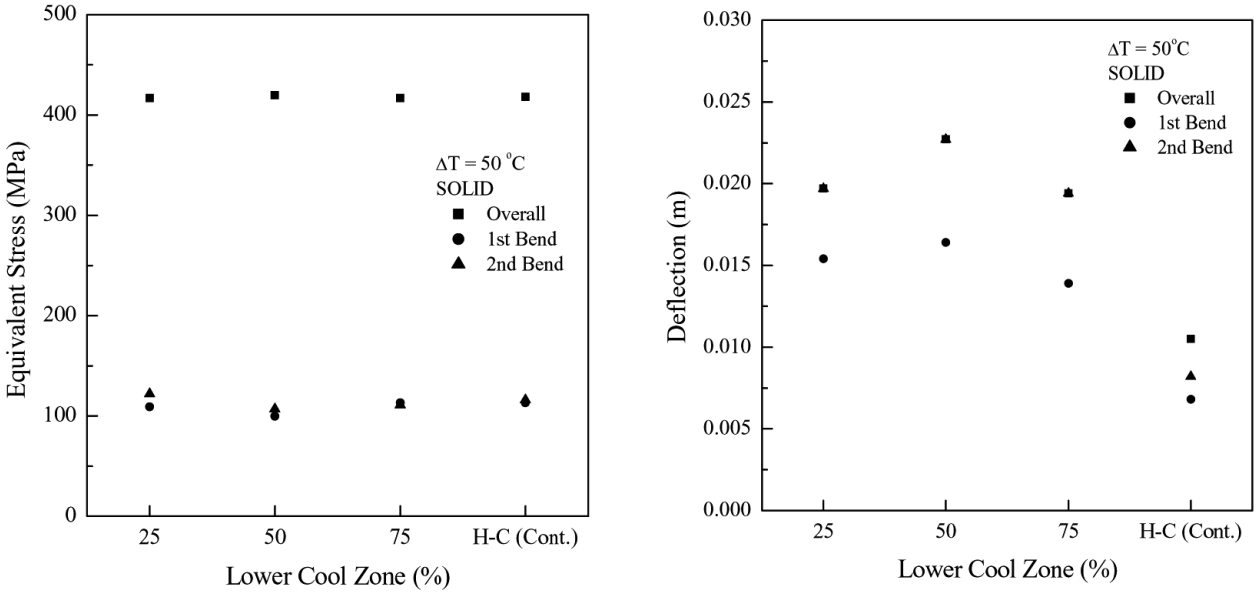

Fig. 11. Comparison of Stresses and Deflections between Various Temperature Distributions due to Thermal Stratification

therefore expected to be the major contributor to the fatigue life of the surge line.

An assessment of fatigue due to thermal stratification and internal pressure was performed assuming a top-to-bottom temperature differential ΔT of 30°C (from the thermal hydraulic analysis) for steady state fluctuation. Steady state fluctuation has the biggest number of cycles (10^6) during the design life and is expected to be the major contributor to fatigue life. The maximum alternative stress in this case is S_a = 324 / 2 = 162 MPa, and from the fatigue curve for austenitic steel [7], the number of cycles is 2×10^6. Therefore, the usage factor (*UF*) is $10^6 / 2 \times 10^6 = 0.5$.

The ASME Section III design curves [7], used above to calculate the cumulative usage factor, are based on tests conducted in laboratory air environments at ambient temperatures applying a margin of 2 on strain and a margin of 20 on cyclic life to account for variations in materials, surface finish, data scatter, and environmental effects (including temperature differences between specimen test conditions and reactor operating experience). However, these design curves lacked sufficient data to explicitly evaluate and account for the degradation attributable to exposure to aqueous coolants. More recent fatigue test data from the United States, Japan, and elsewhere show that the LWR environment can have a significant impact on the fatigue life of carbon and low-alloy steels, austenitic stainless steel, and nickel-chromium-iron (Ni-Cr-Fe) alloys [8].

Therefore, an environmental correction factor (F_{en}) was introduced to account for LWR environments by correcting the fatigue usage calculated with the ASME "air" curves [9]. This method affords the designer greater flexibility to calculate the appropriate impacts for specific environmental parameters.

By definition, F_{en} is the ratio of the fatigue life of the component material in a room temperature air environment to its fatigue life in LWR coolant at operating temperature. To incorporate environmental effects into the fatigue evaluation, the fatigue usage is calculated using provisions set forth in Section III of the ASME Code, and the fatigue design curve is multiplied by the correction factor as $UF_{en} = F_{en} \times UF$. UF_{en} should be less than 1, or $F_{en} \times UF < 1$, which determines the allowable F_{en} as $F_{en} < 1.0 / UF = 1.0 / 0.5 = 2.0$. For the surge line not to fail due to fatigue, the environmental fatigue life correction factor calculated should be less than 2.0 for thermal stratification loading due to the steady state fluctuation conditions.

5. CONCLUSIONS

Finite element models of surge lines were developed using several elements available in a general-purpose commercial program. Stress analyses were performed to obtain the response characteristics due to various thermal stratification loading types, and environmental fatigue

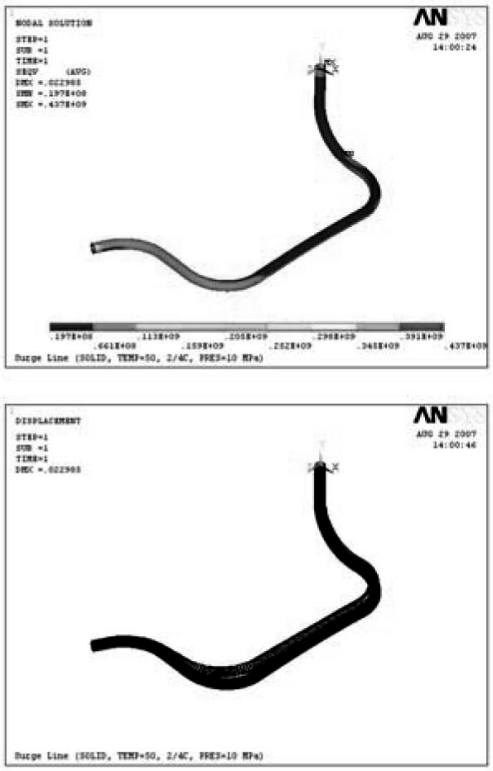

(a) Overall

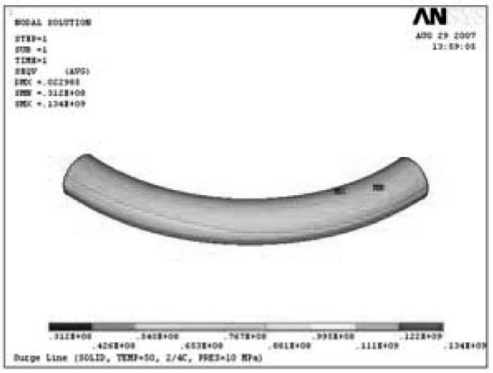

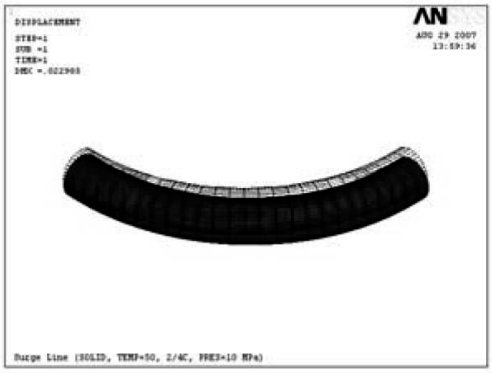

(c) 2nd Bend

Fig. 12. Equivalent Stresses and Deflections due to Thermal Stratification and Internal Pressure

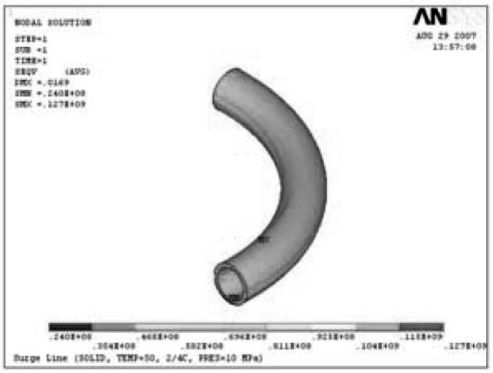

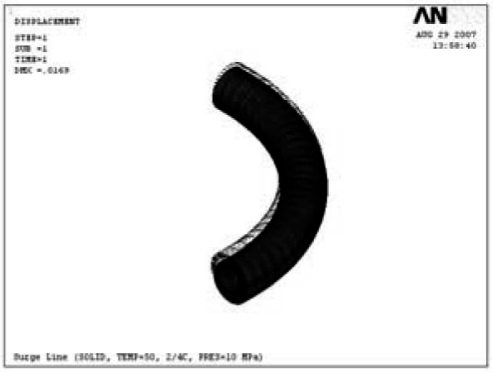

(b) 1st Bend

characteristics were addressed, generating the following conclusions:

- Pipe, shell and solid elements give the same modal characteristics for pipes such as pressurizer surge lines.
- The Pipe element is not appropriate for calculation of the stress in a full model of the surge line due to the internal pressure application method.
- Shell and solid elements generate different stress at the nozzles but the same stress at the elbows due to the differing degrees of freedom imposed on their fixed boundary conditions.
- Applying a top-to-bottom temperature differential in a pipe produces the highest stress in the flange but does not yield conservative stress in the elbows.
- Stress due to thermal stratification is much higher than that due to internal pressure.
- The usage factor due to thermal stratification ΔT=30°C for steady state fluctuation is 0.5 and the allowable environmental correction factor F_{en} in this case should be less than 2.0 to avoid environmental fatigue failure.

REFERENCES

[1] USNRC, Thermal Stresses in Piping Connected to Reactor Coolant Systems, Bulletin No. 88-08, U.S. Nuclear Regulatory

Commission, Washington, DC (1988).
[2] USNRC, Pressurizer Surge Line Thermal Stratification, Bulletin No. 88-11, U.S. Nuclear Regulatory Commission, Washington, DC (1988).
[3] NEA, Thermal Cycling in LWR Components in OECD-NEA Member Countries, NEA/CSNI/R(2005)8, NEA CSNI, CSNI Integrity and Ageing Working Group, Organization for Economic Co-operation and Development (2005).
[4] ANSYS, *ANSYS Structural Analysis Guide*, ANSYS, Inc., Houston (2007).
[5] Grimes, R.G., Lewis, J.G., and Simon, H.D., "A Shifted Block Lanczos Algorithm for Solving Sparse Symmetric Generalized Eigenproblems," *SIAM Journal on Matrix Analysis and Applications*, Vol.15, No.1, pp.228-272 (1994).
[6] Jhung, M.J., Kang, D.G., and Jo, J.C., "Coupled Thermal Hydraulic and Stress Analysis of Pipe with Two Bends," *Transactions of the Korean Society of Pressure Vessels and Piping*, Vol.3, No.2, pp.65-70 (2007).
[7] ASME, ASME Boiler and Pressure Vessel Code, Section III, Appendix I Design Stress Intensity Values, Allowable Stresses, Material Properties, and Design Fatigue Curves, The American Society of Mechanical Engineers (2004).
[8] USNRC, "Guidelines for evaluating fatigue analysis incorporating the life reduction of metal components due to the effects of the light-water reactor environment for new reactors," Regulatory Guide 1.207, U.S. Nuclear Regulatory Commission, Washington, DC (2007).
[9] USNRC, "Effect of LWR Coolant Environments on Fatigue Life of Reactor Materials," NUREG/CR-6909, U.S. Nuclear Regulatory Commission, Washington, DC (2007).